Acta Cryst. (1988). A44, 496–499

Measurement of the Coherence Length of Highly Collimated X-rays from the Visibility of Equal-Thickness Fringes

BY TETSUYA ISHIKAWA

Photon Factory, National Laboratory for High Energy Physics, Oho-machi, Tsukuba-gun, Ibaraki 305, *Japan*

(*Received* 2 *Spetember* 1987; *accepted* 29 *February* 1988)

Abstract

The coherence length of highly collimated X-rays produced by a collimator system, using successive asymmetric reflections, has been determined for the first time from the visibility of equal-thickness fringes in the Laue geometry. Observed transverse and longitudinal components of the coherent length were more than 220 and 40 μm, respectively, at a wavelength of 0·70 Å.

1. Introduction

In most theoretical and experimental studies involving dynamical diffraction of X-rays, the effect of the coherence length has not been taken into consideration. In reality, X-rays must have finite transverse and longitudinal coherence lengths relating to the transverse momentum spread (angular divergence) and the energy divergence. A highly parallel X-ray beam obtained by a single or successive asymmetric diffraction (Kohra & Kikuta, 1968) is known to have a long coherence length in both the transverse and longitudinal components. The angular collimation effect of asymmetric diffraction is expected to make the transverse coherence length longer, and the spatially dispersive nature of such X-ray optical devices makes the longitudinal coherence length longer as well.

Although a single or successive asymmetric diffraction has extensively been used for collimation to obtain intrinsic rocking curves for various cases (Kikuta & Kohra, 1970; Kikuta, 1971) or has been applied to 'plane-wave X-ray topography' (Renninger, 1961; Ishida, Miyamoto & Kohra, 1976), there seems to be no direct evidence that the X-ray beam produced by such an optical device has a longer coherence length. This is mainly because the flux obtained from conventional X-ray sources is insufficient for the direct measurement of the coherence length.

The recent development of synchrotron radiation provides sufficient X-ray flux after monochromatization as well as collimation to enable us to estimate the coherence length directly from the contrast of equal-thickness fringes of a wedge-shaped crystal.

2. Principles

When symmetric diffraction in Laue geometry occurs with a highly collimated X-ray beam incident on a perfect crystal, X-ray wave fields inside the crystal become almost planar and only a small region of dispersion surfaces is excited. The Poynting vectors, $\mathbf{S}_i$ ($i = 1, 2$), of the wave fields belonging to the upper (1) and lower (2) branches of the dispersion surfaces have different directions, as shown in Fig. 1, except when the Bragg condition for symmetrical diffraction is exactly satisfied (Kato, 1958; Ewald, 1958).

In the widely used dynamical theory of X-ray diffraction for an incident plane wave, where the infinitely wide wave front and the infinitely long wave train are implicitly assumed, the field intensity observed at a point P on the exit surface is given by the interference of the two wave fields. One wave field belongs to branch 1 of the dispersion surfaces and propagates along $\mathbf{S}_1$ from point A on the entrance surface, the other belongs to branch 2 and propagates along $\mathbf{S}_2$ from point B (Fig. 2).

However, the wave front always has a finite width and the wave train always has a finite length, regardless of the high collimation of the X-ray beam with

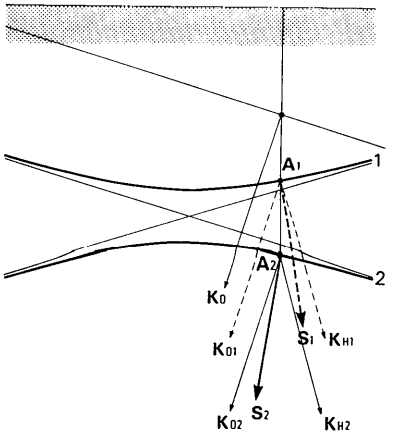

Fig. 1. Dispersion surface for one polarization state. For plane waves, the wave fields from tie points A_1 and A_2 will interfere. Poynting vectors $\mathbf{S}_1$ and $\mathbf{S}_2$ for branches 1 and 2 of the dispersion surface have generally different directions, because they are normal to the respective branches of the dispersion surface.

0108-7673/88/040496-04$03.00

asymmetric diffraction (Renninger, 1961; Kohra, 1962) or the control of a wave fan (Authier, 1960). Accordingly, when the distance between points A and B exceeds a certain critical value, two wave fields propagating along $\mathbf{S}_1$ and $\mathbf{S}_2$ cannot interfere at the point P.

The distance d between points A and B is given by the crystal thickness t and the angle 2Ω between $\mathbf{S}_1$ and $\mathbf{S}_2$, and is represented in a symmetrical diffraction geometry as

$$d = 2t \tan \Omega. \tag{1}$$

The angle Ω is related to the deviation from the exact Bragg condition and calculated from the following equation in the non-absorbing crystal:

$$\tan \Omega = |W| \tan \theta_B/(1+W^2)^{1/2}. \tag{2}$$

Here, θ_B is the Bragg angle and W is a parameter representing the deviation from the exact Bragg condition, and is given as

$$W = 2\delta/\omega_s, \tag{3}$$

where δ is the angular deviation from the exact Bragg condition and ω_s is the angular width of the relevant reflection.

The criterion that the two wave fields from points A and B interfere at point P is given by the visibility of *Pendellösung* fringes at point P. In order to observe *Pendellösung* fringes, a wedge-shaped crystal is used for the sample. How thick the crystal can be for the visibility of *Pendellösung* fringes gives a measure of the coherence length of the incident highly collimated X-rays, although unequal absorption between wave fields 1 and 2 could blur the fringes as the portion of the crystal gets thicker.

If the interference fringes are visible up to the crystal thickness, t_{limit}, at a certain value of W, then we can conclude that the transverse coherence length is longer than d_t and the longitudinal coherence length is longer than d_l, which are

$$d_t = 2t_{\text{limit}}|W| \sin \theta_B/(1+W^2)^{1/2} \tag{4}$$

and

$$d_l = 2t_{\text{limit}}|W| \tan \theta_B \sin \theta_B/(1+W^2)^{1/2}. \tag{5}$$

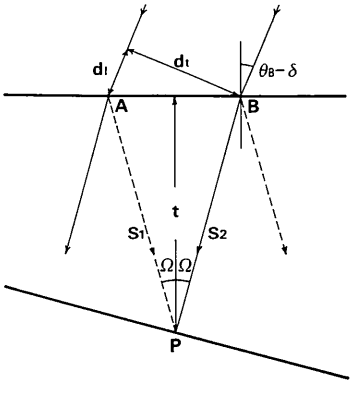

Fig. 2. Optical paths of branch 1 and 2 beams which are responsible for the interference at a point P on the exit surface.

3. Experimental

An arrangement of four crystals, shown schematically in Fig. 3, was set up on Beam Line 15C of the Photon Factory, National Laboratory for High Energy Physics. A horizontal-axis multiple-crystal diffractometer (Ishikawa, Matsui & Kitano, 1986) was used for this arrangement. A (111) floating zone (FZ) silicon pre-monochromator (C_1) was mounted on a water-cooled crystal holder to avoid thermal instability caused by white synchrotron radiation. This crystal was adjusted to reflect $\lambda = 0{\cdot}70$ Å X-rays with symmetric 111 reflection. A slit reduced the beam size of monochromatic X-rays from the pre-monochromator to 35 mm wide × 0·5 mm high. The second (C_2) and third (C_3) crystals were cut from the same FZ silicon boule as the pre-monochromator crystal. Asymmetric 220 and $\bar{2}\bar{2}0$ reflections take place from these crystals. The asymmetric factor, defined by $b = \sin(\theta_B - \alpha)/\sin(\theta_B + \alpha)$, of both crystals was 1/40 at $\lambda = 0{\cdot}70$ Å. Here, α is the angle between net planes and the surface of the crystal. This value was experimentally confirmed for each crystal by measuring the cross section of the beam before and after diffraction. The angular divergence of the beam incident on a sample crystal (S) is

$$\Delta\theta = b_2^{1/2} b_3 \omega_s, \tag{6}$$

where b_i ($i = 2, 3$) is the asymmetric factor of the second and the third crystal (Kohra & Kikuta, 1968). If $b_2 = b_3 = 1/40$ and $\omega_s = 2{\cdot}09''$ arc, then $\Delta\theta$ is estimated to be 0·008″ arc. This is 1/253 smaller than the intrinsic diffraction width of the sample crystal (S) in which symmetric 220 diffraction of silicon takes place. The present arrangement is in a non-dispersive parallel setting, where energy dispersion can be neglected.

The sample crystal was prepared in a wedge-shaped form from the same FZ silicon boule as the crystals

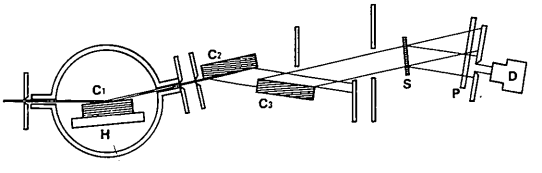

Fig. 3. Experimental arrangement (front view). C_1, fore crystal, (111) silicon, 111 symmetric reflection; C_2 and C_3, collimator crystals, 220 asymmetric reflection of silicon with asymmetric factor 1/40 at $\lambda = 0{\cdot}70$ Å; S, sample crystal, 220 symmetric reflection in the Laue geometry; H, water-cooled crystal holder; P, photographic plate; D, monitoring detector.

discussed previously (Fig. 4). Mechano-chemical polishing was done to remove the damaged layers near the surface. Topographs were taken at five angular positions of the sample crystal, roughly at $\delta = 0{\cdot}0, \pm 1{\cdot}2$ and $\pm 2{\cdot}4''$. In order to avoid the angular integration of diffracted images due to drift of the sample, stability of the X-ray optics was checked by measuring the diffracted intensity from the sample for 30 min before starting each exposure. Also, the diffracted intensity was monitored during the exposure by measuring the intensity of the transmitted beam through a nuclear emulsion plate (Ilford L4, 50 μm thick). With the storage ring at 2·5 GeV and 150 mA beam current, the exposure time ranged from 15 to 80 min.

4. Results and discussion

Fig. 5 shows a set of equal-thickness fringes observed in the diffracted beam at different values of W. On the W scale, the Laue-case reflection curve for a non-absorbing crystal is

$$R_L(W) = \frac{\sin^2[\pi t(1+W^2)^{1/2}/\Delta_0]}{1+W^2}. \qquad (7)$$

For this experiment, only the σ polarization is considered because synchrotron radiation is used. The characteristic *Pendellösung* distance Δ_0 is

$$\Delta_0 = \lambda \cos\theta_B/(\chi_h\chi_{\bar{h}})^{1/2} \qquad (8)$$

and estimated to be 36·51 μm using the calculated value of the polarizability, χ_h (Sasaki, 1984); this includes the correction for the anomalous scattering (Cromer & Liberman, 1981). Δ_0 corresponds to the fringe period at $W = 0$.

When the Bragg condition is exactly satisfied ($W = 0$, Fig. 5C), equal-thickness fringes are visible over the whole area of the present sample crystal with a maximum thickness of 1·4 mm. Although the planned values of deviation from the exact Bragg condition, δ, are $-2{\cdot}4$, $-1{\cdot}2$, 0, 1·2 and 2·4″ for Figs. 5(A) to (E) respectively, a slight shift from these planned values is recognized in the results as the changes of fringe periods are observed. When the Bragg condition is almost satisfied ($W \simeq 0$), small deviations of W from zero will not make noticeable differences in the period of equal-thickness fringes given by

$$T = \Delta_0/(1+W^2)^{1/2}, \qquad (9)$$

whereas even a small deviation from the planned value of non-zero W will result in a large difference in the fringe period. Thus, the W values are redetermined from the observed periods to be (A) $-2{\cdot}39$, (B) $-1{\cdot}13$, (C) 0, (D) 1·07 and (E) 2·28, respectively.

As expected from the consideration of the coherence length, the crystal thickness, $t_{\rm limit}$, to which the equal-thickness fringes are observed becomes smaller

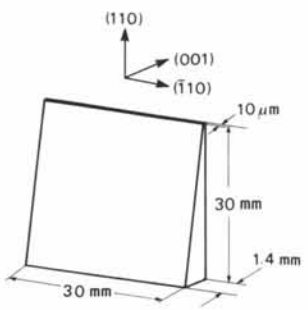

Fig. 4. Shape of the sample crystal. 2$\bar{2}$0 reflection was used to take topographs.

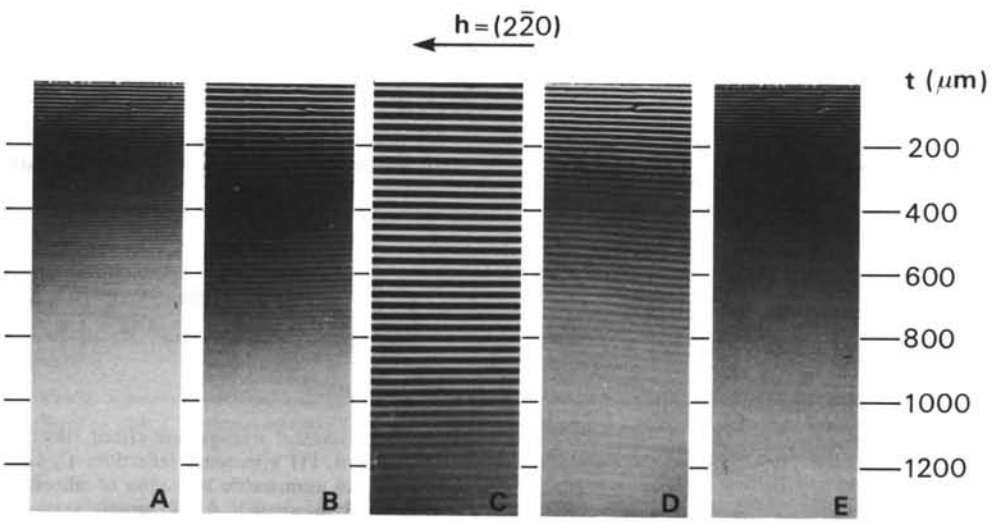

Fig. 5. Equal-thickness fringes observed at W values of (A) $-2{\cdot}39$, (B) $-1{\cdot}13$, (C) 0·0, (D) 1·07 and (E) 2·28.

Table 1. *Calculated X-ray optical path difference, d_t and d_l*

W	t_{limit} (μm)	d_t(μm)	d_l(μm)
−2·39	640	220	41
−1·13	780	220	41
0·0	>1400	—	—
1·07	810	220	41
2·28	650	220	41

as the deviation from the exact Bragg condition becomes larger. The observed values of t_{limit} for each W value, together with the calculated values of d_t and d_l from (4) and (5), are summarized in Table 1. Here, values of t_{limit} were determined by densitometric measurement.

The d_t and d_l values presented here imply that (*a*) the transverse coherence length is longer than d_t and (*b*) the longitudinal coherence length is longer than d_l. Although the visibility of fringe contrast becomes worse as the sample becomes thicker because of the effect of absorption, the two beams incident on points *A* and *B* in Fig. 2 are coherent when interference can be observed at point *P*.

The applicability of the present method is limited to a highly collimated wave, the angular and spectral divergence of which is much less than the rocking-curve width of the sample crystal. Nevertheless, we can show that the coherence length of X-rays produced by the present X-ray optics is fairly long in both longitudinal and transverse directions. This kind of coherent X-rays will enlarge the possibilities of X-ray holography in the hard-X-ray region, although attempts in this direction have been limited to the soft-X-ray region (Aoki & Kikuta, 1974).

Further, the application of the coherent X-rays obtained here to plane-wave X-ray topography is an interesting possibility. Actually, in the present experiment, some contrasts, probably due to so-called micro-defects, are already seen as distortions of the parallel equal-thickness fringes in the upper parts of Figs. 5(*A*) to (*E*) (except in Fig. 5*C*, where the Bragg condition is exactly satisfied). Further analysis of these micro-defect contrasts will be reported elsewhere.

The author expresses his sincere gratitude to Professors K. Kohra, M. Ando and S. Kikuta for valuable advice, fruitful discussions, and continuous encouragement. This work was performed using the synchrotron radiation facility of the Photon Factory, National Laboratory for High Energy Physics, under Proposal No. 87-100.

References

AOKI, S. & KIKUTA, S. (1974). *Jpn. J. Appl. Phys.* **13**, 1385-1392.
AUTHIER, A. (1960). *C. R. Acad. Sci.* **251**, 2502.
CROMER, D. T. & LIBERMAN, D. A. (1981). *Acta Cryst.* A**37**, 267-268.
EWALD, P. P. (1958). *Acta Cryst.* **11**, 888-891.
ISHIDA, H., MIYAMOTO, N. & KOHRA, K. (1976). *J. Appl. Cryst.* **9**, 240-241.
ISHIKAWA, T., MATSUI, J. & KITANO, T. (1986). *Nucl. Instrum. Methods*, A**246**, 613-616.
KATO, N. (1958). *Acta Cryst.* **11**, 885-887.
KIKUTA, S. (1971). *J. Phys. Soc. Jpn*, **30**, 222-227.
KIKUTA, S. & KOHRA, K. (1970). *J. Phys. Soc. Jpn*, **29**, 1322-1328.
KOHRA, K. (1962). *J. Phys. Soc. Jpn*, **17**, 589-590.
KOHRA, K. & KIKUTA, S. (1968). *Acta Cryst.* A**24**, 200-205.
RENNINGER, M. (1961). *Z. Naturforsch. Teil A*, **16**, 1110-1111.
SASAKI, S. (1984). *Anomalous Scattering Factors for Synchrotron Radiation Users, Calculated Using Cromer and Liberman's Method.* KEK Report 83-22. National Laboratory for High Energy Physics, Japan.

Acta Cryst. (1988). A**44**, 499-506

On the Use of Least-Squares Restraints for Origin Fixing in Polar Space Groups

BY H. D. FLACK

Laboratoire de Cristallographie aux Rayons X, Université de Genève, 24 quai Ernest Ansermet, CH-1211 Genève 4, Switzerland

AND D. SCHWARZENBACH

Institut de Cristallographie, Université de Lausanne, BSP Dorigny, CH-1015 Lausanne, Switzerland

(*Received* 12 *October* 1987; *accepted* 8 *March* 1988)

Abstract

The theory of fixing the origin of the coordinate system in a polar space group by use of restraints (soft constraints or pseudo-observations) is developed for any space group in any setting. The coefficients of the optimal restraint equation are on the average proportional to the square of the atomic numbers. They are determined directly from the unrestrained singular normal-equations matrix. Application of the restraint results in a positive-definite matrix which is as nearly diagonal as possible for the atomic

0108-7673/88/040499-08$03.00